

Spectral neighbor joining for reconstruction of latent tree models

Ariel Jaffe¹, Noah Amsel¹, Boaz Nadler², Joseph T. Chang³, and Yuval Kluger^{1,4,5}

¹*Program in Applied Mathematics, Yale University, New Haven, CT 06511*

²*Department of Computer Science, Weizmann Institute of Science, Rehovot, 76100, Israel*

³*Department of Statistics, Yale University, New Haven, CT 06520, USA*

⁴*Interdepartmental Program in Computational Biology and Bioinformatics, New Haven, CT 06511*

⁵*Department of Pathology, New Haven, CT 06511*

Abstract

A key assumption in multiple scientific applications is that the distribution of observed data can be modeled by a latent tree graphical model. An important example is phylogenetics, where the tree models the evolutionary lineages of various organisms. Given a set of independent realizations of the random variables at the leaves of the tree, a common task is to infer the underlying tree topology. In this work we develop Spectral Neighbor Joining (SNJ), a novel method to recover latent tree graphical models. In contrast to distance based methods, SNJ is based on a spectral measure of similarity between all pairs of observed variables. We prove that SNJ is consistent, and derive a sufficient condition for correct tree recovery from an estimated similarity matrix. Combining this condition with a concentration of measure result on the similarity matrix, we bound the number of samples required to recover the tree with high probability. We illustrate via extensive simulations that SNJ requires fewer samples to accurately recover trees in regimes where the tree contains a large number of leaves or long edges. We provide theoretical support for this observation by analyzing the model of a perfect binary tree.

1 Introduction

Learning the structure of an unobserved tree graphical model is a fundamental problem in many scientific domains. For example, phylogenetic tree reconstruction methods are applied to infer the evolutionary history of different organisms, see [10, 46] and references therein. In machine learning, applications of latent tree models include estimation of human interactions, medical diagnosis and classification of documents [31, 19].

As described in Section 2, in tree based graphical models, each node of the tree has an associated random variable. In many applications one can only observe the values at the terminal nodes of the tree, while the structure of the tree, as well as the values at the internal nodes, are unknown. Given a set of independent realizations of the observed variables, a common task is to infer the tree structure. In phylogeny, the terminal nodes correspond to current species, also known as taxa, and the hidden nodes correspond to their common ancestors. For every taxa, one is given a string of characters, such as a DNA or protein sequence. The task is to infer a tree that characterizes the evolutionary lineages of the organisms [13, 9].

Many algorithms have been developed to recover the latent tree structure from observed data. These include distance based methods such as the classic neighbor joining (NJ) [40] and UPGMA [44], maximum

parsimony [5, 14], maximum likelihood [12, 17, 45, 38], quartets and meta trees [1, 48, 35, 43, 39, 23], and Bayesian methods [36]. Other approaches for tree recovery are based on a measure of statistical dependency between pairs of terminal nodes, see [35, 19]. As reviewed in [54, 24], each one of these approaches has different strengths and weaknesses.

Of particular relevance to our work is the neighbor joining algorithm, one of the most important methods derived in phylogeny. Due to its simplicity and scalability, neighbor joining is widely used in practice, and often serves as a baseline when testing new methods for reconstruction of evolutionary trees [28, 18, 51, 15]. For completeness, this approach is briefly outlined in Section 3.2. Due to its importance, several works investigated the theoretical properties of the neighbor joining algorithm. Atteson [2] studied its consistency and derived a sufficient condition for correct tree recovery by NJ. A different guarantee for exact recovery was derived in [29], via a link between NJ and quartet-based methods. Additional theoretical properties of NJ were studied in [16, 4, 15, 34]. As discussed in several works [26, 50, 47], to recover certain tree topologies or trees with a large number of terminal nodes, NJ may require a very large number of samples.

Our contribution In this work we derive spectral NJ, a novel method to reconstruct tree graphical models. In contrast to NJ, which is based on a distance measure between observed nodes, our approach, described in Section 3.3, is based on the spectral structure of a similarity matrix of all pairs of observed nodes. The key property we use is the conditional independence of a node from the rest of the tree, given the values of its immediate neighboring nodes. As we prove in Lemma 3.1, this implies a rank one structure on certain matrices, similar to our previous works on other latent variable models [21, 20, 22, 33]. In section 5.1 we show that our spectral criterion for joining subsets of nodes is intimately related to quartet based approaches for reconstructing trees. Loosely speaking, at each step SNJ merges the two subsets whose sum of all quartet tests is most consistent with the tree topology. On the theoretical front, in Section 4.1 we prove the consistency of SNJ, given an exact similarity matrix. Furthermore, in Lemma 4.7 we derive a sufficient condition on the difference between the exact and estimated similarity matrices that guarantees perfect recovery of the tree. Next, Lemma 4.8 provides a concentration of measure result on the estimated similarity matrix in the case of the Jukes-Cantor model, a popular model of sequence evolution [25]. Subsequently, in Theorem 4.2 we derive a lower bound on the required number of samples for SNJ to correctly recover the underlying tree under this model.

We note that Lemma 4.7 is analogous to the classic result obtained by Atteson in [2, Theorem 4] for correct tree reconstruction by the NJ algorithm. We compare the two sufficient conditions for the specific case of a perfect binary tree with equal distances between all adjacent nodes. For this model, we show that our sufficient condition is less strict than the analogous one for the classical NJ. Consequently, we anticipate SNJ to recover the correct tree structure with a smaller number of samples. Indeed, in Section 6 we illustrate, via extensive simulations, the improved accuracy in reconstruction of SNJ over the classical NJ under a variety of simulated settings.

In summary, the proposed SNJ method has several desirable properties, similar to NJ, including consistency, scalability to large trees and simplicity of implementation. Furthermore, as we show both theoretically and via simulations, SNJ outperforms NJ under various scenarios of relevance to biological applications.

2 Problem setup

Let \mathcal{T} be an unrooted bifurcating tree with m terminal nodes. In such a tree, the leaves or terminal nodes have a single neighbor, while internal nodes have three neighbors. We assume that each node of the tree has an associated discrete random variable attaining values in the set $\{1, \dots, d\}$. We denote by $\mathbf{x} = (x_1, \dots, x_m)$

the vector of random variables at the m observed terminal nodes of the tree, and by h_A, h_B etc. the random variables at the internal nodes. We assume that these random variables form a Markov random field on \mathcal{T} . This means that given the value of its neighbors, the random variable at each node is statistically independent of the rest of the tree. An edge $e(h_A, h_B)$ connecting the pair of adjacent nodes (h_A, h_B) is equipped with two transition matrices of size $d \times d$,

$$P(h_A|h_B)_{ab} = \Pr[h_A = a|h_B = b] \quad P(h_B|h_A)_{ba} = \Pr[h_B = b|h_A = a]. \quad (1)$$

Our observed data is a matrix $X = [\mathbf{x}^{(1)}, \dots, \mathbf{x}^{(n)}] \in \{1, \dots, d\}^{m \times n}$, where $\mathbf{x}^{(j)}$ are random i.i.d. realizations of the observed variables at the m terminal nodes of the tree. Each row in the matrix is a sequence of length n that corresponds to a terminal node in the tree, see illustration in Figure 1. For example, in phylogeny, each row in the matrix corresponds to a different species, while each column corresponds to a different location in a DNA or protein sequence. The latent nodes in the tree correspond to the common ancestors of different subsets of the observed organisms, see [10] and references therein.

Given the matrix X , the task at hand is to recover the structure of the tree \mathcal{T} . For the tree to be identifiable, we assume that for every pair of adjacent nodes h_A, h_B , the corresponding $d \times d$ stochastic matrices $P(h_A|h_B)$ and $P(h_B|h_A)$ defined in (1) are full rank, with determinants that satisfy

$$0 < \delta < |P(h_A|h_B)| < \xi < 1 \quad 0 < \delta < |P(h_B|h_A)| < \xi < 1. \quad (2)$$

Eq. (2) implies that all edge transition matrices are invertible and are not permutation matrices. These are critical conditions for identifiability of the tree topology, see Proposition 3.1 in [6] and [30]. We remark that though our approach can be applied to recover the topology of *rooted trees* as well as unrooted ones, determining the location of the root requires additional assumptions, see [42].

3 The spectral neighbor joining algorithm

To introduce our novel spectral approach, in Section 3.1 we first present known measures for similarity and distance between nodes in a latent tree model. For completeness, Section 3.2 briefly describes the standard neighbor joining algorithm. In Section 3.3 we derive a new spectral criterion for neighbor joining and present our algorithm in detail.

3.1 The symmetric affinity and distance matrices

We denote by $P(x_i|x_j)$ the stochastic matrix containing the distribution of x_i given x_j . By the tree model, $P(x_i|x_j)$ is the product of the stochastic matrices of the edges along the directed path from x_i to x_j . For example, in the tree shown in Figure 1, the hidden nodes on the path from x_1 to x_3 are h_C and h_A . Thus,

$$P(x_1|x_3) = P(x_1|h_C)P(h_C|h_A)P(h_A|x_3).$$

To obtain a symmetric measure of similarity between nodes, we denote by $r(x_i, x_j)$ the *symmetric affinity* between a pair of terminal or hidden nodes,

$$r(x_i, x_j) = \sqrt{|P(x_i|x_j)||P(x_j|x_i)|}, \quad r(h_A, h_B) = \sqrt{|P(h_A|h_B)||P(h_B|h_A)|}. \quad (3)$$

Here $|P(x_i|x_j)|$ denotes the determinant of the matrix $P(x_i|x_j)$. Let $R \in \mathbb{R}^{m \times m}$ denote the symmetric affinity matrix between all pairs of terminal nodes,

$$R(i, j) = r(x_i, x_j) = \sqrt{|P(x_i|x_j)||P(x_j|x_i)|}. \quad (4)$$

An important property of $R(i, j)$ is that it is *multiplicative* along the path between x_j and x_i . For example, in Figure 1, the affinity between x_1 and x_3 is equal to

$$\begin{aligned} R(1, 3) &= \sqrt{|P(x_1|h_C)||P(h_C|h_A)||P(h_A|x_3)|} \sqrt{|P(x_3|h_A)||P(h_A|h_C)||P(h_C|x_1)|} \\ &= \sqrt{|P(x_1|h_C)||P(h_C|x_1)|} \sqrt{|P(h_A|h_C)||P(h_C|h_A)|} \sqrt{|P(x_3|h_A)||P(h_A|x_3)|} \\ &= r(x_1, h_C)r(h_C, h_A)r(h_A, x_3). \end{aligned}$$

The following symmetric distance between terminal nodes was derived in [7] and [27],

$$D(i, j) = -\log(r(x_i, x_j)). \quad (5)$$

Eq. (5) was used in several distance based methods for reconstructing trees, see [32, 41] and references therein. Note that the log transformation in (5) yields a distance measure between two observed nodes x_i, x_j that is additive along the path connecting them. The additive property is a necessary condition for the consistency of any distance based method [6, 7].

3.2 Background: the neighbor joining algorithm

To motivate our approach, we first briefly describe the classical neighbor joining algorithm [40]. The input to NJ is a matrix $\hat{D} \in \mathbb{R}^{m \times m}$ of estimated distances between observed nodes. NJ iteratively reconstructs the tree via the following procedure:

1. Compute the Q criterion between all pairs,

$$Q(i, j) = (m - 2)\hat{D}(i, j) - \sum_{k \neq \{i, j\}} \hat{D}(k, i) - \sum_{k \neq \{i, j\}} \hat{D}(k, j). \quad (6)$$

2. Reconstruct the tree by repeating the following two steps, until there are three nodes left:

I identify the pair (\hat{i}, \hat{j}) that minimizes the Q criterion,

$$(\hat{i}, \hat{j}) = \underset{i, j}{\operatorname{argmin}} Q(i, j).$$

II merge the pair (\hat{i}, \hat{j}) into a single node l , and update the Q criterion by

$$Q(k, l) = \frac{1}{2}(Q(k, \hat{i}) + Q(k, \hat{j})) \quad \forall k. \quad (7)$$

The neighbor joining method is *consistent*. Namely, if the estimated matrix \hat{D} is sufficiently close to the true distance matrix D , the method is guaranteed to reconstruct the correct tree. As proved by [2], a sufficient condition for recovering the tree is

$$\max_{i, j} |D(i, j) - \hat{D}(i, j)| \leq \frac{d_{\min}}{2}, \quad (8)$$

where d_{\min} is the minimal distance between all pairs of adjacent nodes. The distance between adjacent nodes is defined similarly to the distance between terminal nodes in Eq. (5).

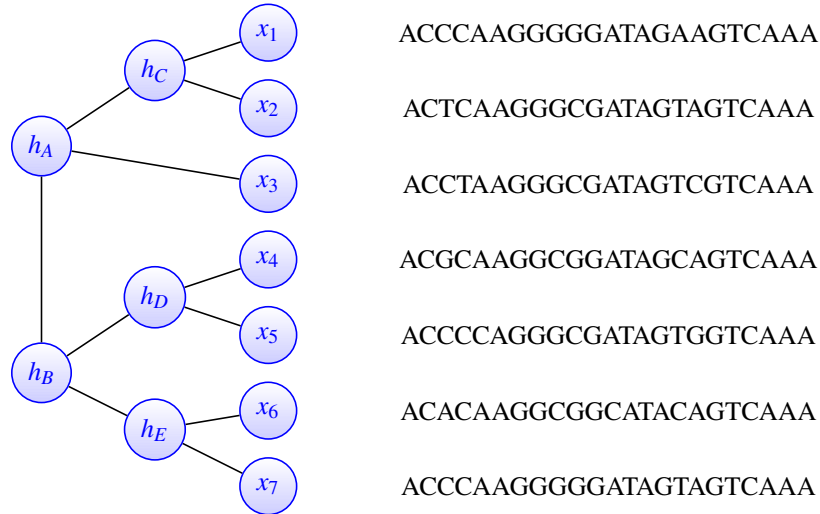


Figure 1: A tree with $m = 7$ observed nodes. In a typical phylogenetic application, the data consists of a sequence of characters for every terminal node.

3.3 A spectral criterion for neighbor joining

To describe our approach, we use the terminology of unrooted trees provided by [53]. We define a *clan* of nodes in \mathcal{T} as a subset of nodes that can be separated from the rest of the tree by removing a single edge. For example, in Figure 1 the subset (x_1, x_2, h_C) forms a clan. Let A and B be two disjoint subsets of $[m]$ such that $\{x_i\}_{i \in A}$ and $\{x_j\}_{j \in B}$ each form the set of terminal nodes of two different clans. We say that A and B are *adjacent subsets* if their union is equal to the terminal nodes of a larger clan. Otherwise, we say that A and B are non adjacent.

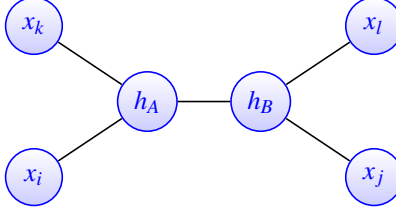
Equipped with these definitions, we describe the spectral neighbor joining approach. In contrast to previous methods that use the symmetric distance (5) or other distance measures, our approach is based on the symmetric affinity matrix between terminal nodes R . Let A be a subset of $\{1, \dots, m\}$ with size $|A| \geq 2$. We denote by R^A the submatrix of R that contains all the affinities $R(i, j)$ with $i \in A$ and $j \in A^c$, where A^c is the complement of A . Lemma 3.1 sets the theoretical foundation for our approach.

Lemma 3.1. *The matrix R^A is rank-one if and only if the subset $\{x_i\}_{i \in A}$ is equal to the terminal nodes of a clan in \mathcal{T} .*

By Lemma 3.1, two nodes x_i and x_j are adjacent if and only if their affinities $r(i, k)$ to all other observed nodes are identical up to a multiplicative factor. This will be a crucial property in developing our spectral neighbor joining algorithm. The proof of Lemma 3.1 relies on the following lemma which is proven in the appendix.

Lemma 3.2. *The following two statements are equivalent:*

1. *The subset $\{x_i\}_{i \in A}$ is equal to the terminal nodes of a clan in \mathcal{T} .*
2. *All quartets of terminal nodes $i, k \in A$ and $j, l \in A^c$ have a topology as in Figure 2, whereby (i, k) and (j, l) are adjacent.*


 Figure 2: A subtree with $m = 4$ observed nodes.

Proof of Lemma 3.1. Suppose that $\{x_i\}_{i \in A}$ consists of the terminal nodes of a clan in \mathcal{T} . Let $e(h_A, h_B)$ be the edge that separates the clan from the rest of the tree, such that all paths between nodes $x_i \in A$ and $x_j \in A^c$ pass through $e(h_A, h_B)$. By the multiplicative property of $R(i, j)$, for all $i \in A, j \notin A$

$$R(i, j) = r(x_i, h_A)r(h_A, h_B)r(h_B, x_j).$$

Let \mathbf{u}_A denote a vector of size $|A|$, whose elements are the affinities between h_A and x_i for $i \in A$. Similarly, let \mathbf{u}_B be a vector of size $m - |A|$ whose elements are the affinities between h_B and x_j for $j \notin A$. Then R^A is equal to

$$R^A = r(h_A, h_B)\mathbf{u}_A\mathbf{u}_B^T. \quad (9)$$

Eq. (9) implies that R^A is rank 1.

Now suppose that $\{x_i\}_{i \in A}$ is not equal to the terminal nodes of a clan. By part 2 of Lemma 3.2, this implies that there is at least one quartet of nodes, $(i, j) \in A$ and $(k, l) \in A^c$ with a structure as in Figure 2. Let R_{ij}^{kl} be the 2×2 submatrix of R^A that contains the pairwise affinities between i, j and k, l . Then its determinant is

$$\begin{aligned} |R_{ij}^{kl}| &= R(i, k)R(j, l) - R(i, l)R(j, k) = r(x_i, h_A)r(h_A, x_k)r(x_j, h_B)r(h_B, x_l) \\ &\quad - r(x_i, h_A)r(h_A, h_B)r(h_B, x_l)r(x_j, h_B)r(h_A, h_B)r(h_A, x_k) \\ &= r(x_i, h_A)r(h_A, x_k)r(x_j, h_B)r(h_B, x_l)(1 - r(h_A, h_B))^2. \end{aligned} \quad (10)$$

Combining Eq. (2) with $r(x_i, x_j)$ in Eq. (3) implies that all terms in Eq. (10) are bounded away from zero and hence R_{ij}^{kl} is full rank. Since R_{ij}^{kl} is a submatrix of R^A , it follows that R^A is at least rank two. \square

Lemma 3.1 implies that given perfect knowledge of R , we can infer if A is equal to the terminal nodes of a clan by computing the rank of R^A . In practice, we typically only have a noisy estimate of the entries of R . Then, all submatrices are full rank, though for the correct subsets they are approximately rank 1. Accordingly, instead of the rank, our criterion whether to join two subsets A_i and A_j is based on the second largest singular value of $R^{A_i \cup A_j}$. This $(|A_i| + |A_j|) \times (m - |A_i| - |A_j|)$ sized matrix contains the affinities between terminal nodes in $A_i \cup A_j$ and the remaining nodes. We denote its second largest singular value by $\sigma_2(R^{A_i \cup A_j})$. Specifically, SNJ recovers the tree by performing the following operations:

- Set $A_i = \{i\}$ for all i . Compute a matrix $\Lambda \in \mathbb{R}^{m \times m}$ where

$$\Lambda(i, j) = \sigma_2(R^{A_i \cup A_j}).$$

- Repeat the following two steps until only three subsets remain.

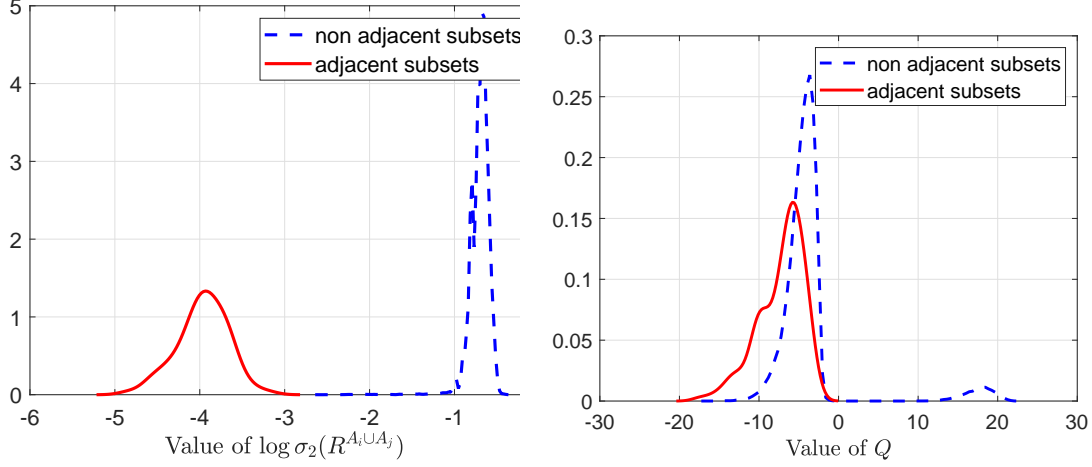


Figure 3: The orange and blue lines are the empirical distributions of $\sigma_2(R^{A_i \cup A_j})$ for the spectral neighbor joining (left), and the Q parameter for neighbor joining (right), for cases where A_i, A_j are adjacent and non adjacent pairs of subsets with size 1.

I Identify the pair (\hat{i}, \hat{j}) that minimizes $\Lambda(i, j)$,

$$(\hat{i}, \hat{j}) = \underset{ij}{\operatorname{argmin}} \Lambda(i, j). \quad (11)$$

II Merge $A_{\hat{i}}, A_{\hat{j}}$ into a subset $A_l = A_{\hat{i}} \cup A_{\hat{j}}$. Update the Λ criterion via

$$\Lambda(k, l) = \sigma_2(R^{A_k \cup A_l}) \quad \forall k. \quad (12)$$

As we can see SNJ has a similar algorithmic structure as NJ, with the key difference being the use of the second singular value instead of the Q -criteria. Hence, it is interesting to compare the power of these two test statistics to distinguish between adjacent and non-adjacent terminal nodes. To this end, we generated a random Jukes-Cantor tree model with $m = 512$ terminal nodes, associated with random variables with support of $d = 4$ characters. The topology of the tree was generated by the following process: Given m nodes, we merge a pair of random terminal nodes and replace them with a single non-terminal node. Next, we merge another pair of random nodes, either terminal or non terminal and again replace them with a single non-terminal node. We continue with this process until three nodes remain, and we connect them to a non terminal node. We set the mutation rates between adjacent nodes to be 10% and the number of realizations to be $n = 500$. The left panel of Figure 3 shows the empirical distribution of $\log \sigma_2(R^{A_i \cup A_j})$ at the first SNJ iteration, where $A_i = \{i\}$ for all i . The right panel shows the empirical distribution of the NJ Q criterion in Eq. (6). The red and blue lines correspond to pairs of adjacent and non-adjacent terminal nodes, respectively. Comparing the two panels, we clearly see that adjacent pairs can be perfectly separated from non-adjacent pairs by their σ_2 values, whereas Q values of adjacent and non-adjacent pairs have a significant overlap. As we will illustrate in Section 6, this better separation of σ_2 vs. the Q -criterion allows SNJ to accurately reconstruct trees from fewer number of samples, where NJ fails.

4 Analysis

In this section we present a theoretical analysis of the SNJ algorithm. First, in section 4.1 we prove consistency of SNJ in the population setting, assuming Eq. (2) holds. Next, we derive a sufficient condition on the difference between the estimated and exact affinity matrices, that guarantees correct tree reconstruction by SNJ. Finally, we derive an explicit expression for the number of samples that guarantees exact tree reconstruction by SNJ with high probability, under the Jukes-Cantor model. Proofs of auxiliary lemmas stated in this section appear in the appendix.

4.1 Consistency of SNJ in the population setting

For SNJ to correctly recover the tree structure, at each iteration it must merge two adjacent subsets of terminal nodes. The following theorem characterizes the second eigenvalue criterion in Eq. (12), depending on whether two subsets are adjacent or not.

Theorem 4.1. *Let $C = A \cup B$, where A and B are disjoint subsets of terminal nodes such that each form a clan in \mathcal{T} . (i) If A, B are adjacent then*

$$\sigma_2(R^C) = 0.$$

(ii) *If A, B are non adjacent then*

$$\sigma_2(R^C) \geq \begin{cases} \frac{1}{2}(2\delta^2)^{\log_2(m/2)}\delta(1-\xi^2) & \delta^2 \leq 0.5, \\ \delta^3(1-\xi^2) & \delta^2 > 0.5. \end{cases} \quad (13)$$

For future use we define

$$f(m, \delta, \xi) = \frac{1}{2}(2\delta^2)^{\log_2(m/2)}\delta(1-\xi^2). \quad (14)$$

Theorem 4.1 has several important implications, which we now discuss. First, as stated in the following corollary, it implies that SNJ is consistent.

Corollary 4.1. *Let \mathcal{T} be a tree which satisfies Eq. (2). Then, SNJ with the exact affinity matrix R is consistent and perfectly recovers \mathcal{T} .*

To see why the corollary is true, recall that at each iteration, SNJ merges two subsets with the smallest value of $\sigma_2(R^{A_i \cup A_j})$. By Theorem 4.1, two adjacent subsets have $\sigma_2 = 0$, whereas if the subsets are non-adjacent, the second singular value corresponding to their union is strictly positive. Hence, given the exact affinity matrix, SNJ merges only adjacent subsets till perfect reconstruction of the whole tree.

A second important implication of Theorem 4.1 is that the bound in Eq. (13) yields insights into the ability of SNJ to correctly recover trees, depending on the number of observed nodes m and parameters δ, ξ . Figure 4 shows the lower bound on $\sigma_2(R^C)$ for non-adjacent subsets in Eq. (13), as a function of δ for $m = 4, 8, 64, 128$, with $\xi = 0.95$. Note that for $m = 4$ the formulas for $\delta^2 \leq 0.5$ and $\delta^2 > 0.5$ coincide. For $\delta^2 \leq 0.5$, which in a phylogenetic setting implies a high mutation rate, the bound decreases with a larger number of terminal leaves m . This implies that SNJ requires a higher number of samples to learn larger trees.

We remark that in general, the lower bounds in Eq. (13) are tight, up to a multiplicative factor of $1/\delta(1+\xi)$, as described in the following lemma.

Lemma 4.1. *For $\delta^2 \leq 0.5$, there exists a tree and two non-adjacent subsets A, B , such that $\sigma_2(R^{A \cup B}) = f(m, \delta, \xi)/\delta(1+\xi)$. For $\delta^2 > 0.5$, there exists a tree with $m = 4$ nodes for which $\sigma_2(R^{A \cup B}) = \delta^3(1-\xi^2)/\delta(1+\xi) = \delta^2(1-\xi)$.*

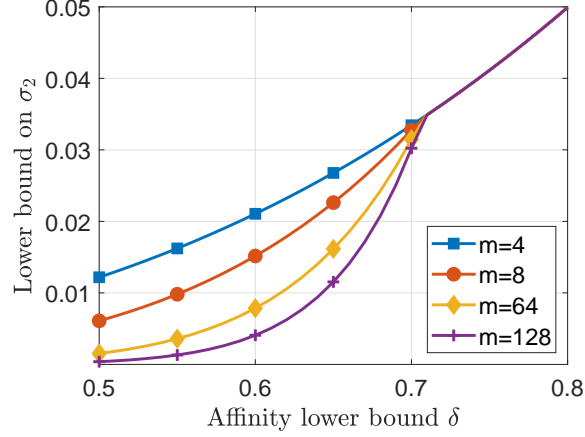


Figure 4: The lower bound (13) on the second largest eigenvalue of $R^{A \cup B}$ for non adjacent subsets A, B as a function of the affinity lower bound δ , at a fixed value $\xi = 0.95$.

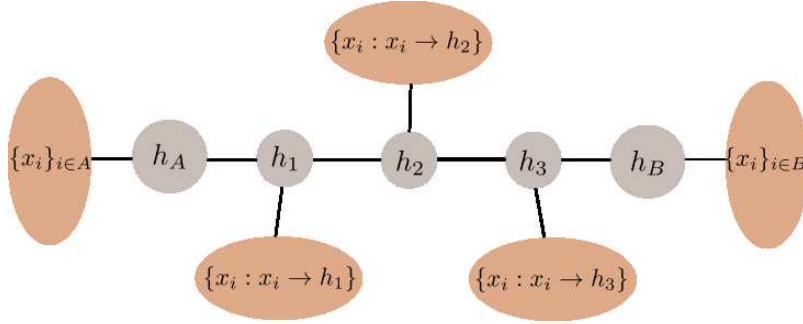


Figure 5: An example of two non adjacent subsets A and B . Every observed node in $(A \cup B)^c$ is assigned to the closest node on the path between h_A and h_B .

The first part of Theorem 4.1 follows directly from Lemma 3.1. To prove the second part, we first introduce some notations and auxiliary lemmas. Let A, B be two non adjacent subsets in \mathcal{T} . We denote by h_A and h_B the corresponding root nodes of A and B , respectively. Since A, B are not adjacent, there are at least two additional hidden nodes on the path between h_A and h_B . Let h_1, \dots, h_l denote the l hidden nodes on this path, see Fig. 5 for an example with $l = 3$ intermediate nodes. We split the remaining $m - |A| - |B|$ terminal nodes to l subsets as follows: Every terminal node in $(A \cup B)^c$ is assigned to the closest hidden node on the path between h_A and h_B (see Fig. 5). The matrix R^C can be rearranged in the following block structure,

$$R^C = \begin{bmatrix} R_1^A & R_2^A & \dots & R_l^A \\ R_1^B & R_2^B & \dots & R_l^B \end{bmatrix} = [R_1 \ R_2 \ \dots \ R_l], \quad (15)$$

where R_i^A is a matrix of $|A|$ rows with the pairwise affinities between the nodes in A and the terminal nodes assigned to h_i . The matrix R_i^B with $|B|$ rows is defined similarly. The matrix R_i is the concatenation of R_i^A and R_i^B . The following lemma shows that this block structure implies that the matrix R^C has rank at most 2.

Lemma 4.2. *Let R^C be the matrix of Eq. (15). Then $1 \leq \text{rank}(R^C) \leq 2$.*

Proof of Lemma 4.2. Recall that R^A denotes the affinity matrix between $\{x_i\}_{i \in A}$ and $\{x_j\}_{j \in A^c}$. Under the assumption that A forms the terminal nodes of a clan, by Lemma 3.1, R^A has rank one. The upper part of R^C which includes $\{R_i^A\}_{i=1}^l$ is a submatrix of R^A and hence has rank one as well. Similarly, the lower part of R^C , which includes $\{R_i^B\}_{i=1}^l$ is a submatrix of R^B and also has rank one. The concatenation of two rank one matrices is at most rank two. \square

Next, we present two auxiliary lemmas. The first concerns rank-2 matrices.

Lemma 4.3. *Let M be a rectangular matrix with $1 \leq \text{rank}(M) \leq 2$, and let $\sigma_2(M)$ be its second singular value. Then*

$$\sigma_2(M)^2 \geq \frac{1}{2} \frac{\|M\|_F^4 - \|M^T M\|_F^2}{\|M\|_F^2}. \quad (16)$$

The next auxiliary lemma expresses $\|R^C\|_F^4 - \|(R^C)^T R^C\|_F^2$ in terms of the norms of the individual blocks R_i^A, R_i^B of the matrix R^C .

Lemma 4.4. *Let R^C be the matrix of Eq. (15) with blocks R_i^A and R_i^B . Then*

$$\|R^C\|_F^4 - \|(R^C)^T R^C\|_F^2 = \sum_{j=1}^l \sum_{k=1}^l (\|R_j^A\|_F \|R_k^B\|_F - \|R_j^B\|_F \|R_k^A\|_F)^2. \quad (17)$$

Proof of Theorem 4.1, part (ii). Let \mathbf{u}_A be the vector of affinities between h_A and nodes in A , and \mathbf{u}_B be the vector of affinities between h_B and B ,

$$\mathbf{u}_A = \{r(x_i, h_A)\}_{i \in A}, \quad \mathbf{u}_B = \{r(x_j, h_B)\}_{j \in B}. \quad (18)$$

Similarly, let \mathbf{v}_j be a vector of affinities between h_j and the terminal nodes associated with it. By the multiplicative property of the affinity $r(x_i, x_j)$, the blocks R_i^A and R_j^B that are part of the matrix R^C in (15) have the following form,

$$R_i^A = \mathbf{u}_A r(h_A, h_i) \mathbf{v}_i^T \quad R_i^B = \mathbf{u}_B r(h_B, h_i) \mathbf{v}_i^T, \quad (19)$$

where $r(h_A, h_i)$ is the affinity between the hidden nodes h_A and h_i . The proof of the theorem is composed of the following three steps:

1. Lower bound $\sigma_2(R^{A \cup B})$ in terms of $\|R_i^A\|_F$ and $\|R_i^B\|_F$.
2. Expand $\|R_i^A\|_F$ and $\|R_i^B\|_F$ in terms of $\|\mathbf{u}_A\|$, $\|\mathbf{u}_B\|$ and $\|\mathbf{v}_i\|$.
3. Lower bound $\|\mathbf{u}_A\|$, $\|\mathbf{u}_B\|$ and $\|\mathbf{v}_i\|$ as a function of m, ξ, δ .

Step 1: Combining lemmas 4.2, 4.3 and lemma 4.4 gives that

$$\sigma_2(R^C) \geq \frac{\sum_{j=1}^l \sum_{k=1}^l (\|R_j^A\|_F \|R_k^B\|_F - \|R_j^B\|_F \|R_k^A\|_F)^2}{\|R^C\|_F^2}.$$

Step 2: We express $\|R_i^A\|_F$ and $\|R_i^B\|_F$ in terms of $\|\mathbf{u}_A\|$, $\|\mathbf{u}_B\|$ and $\|\mathbf{v}_i\|$. This step follows directly from Eq. (19),

$$\|R_i^A\|_F = r(h_A, h_i) \|\mathbf{u}_A\| \|\mathbf{v}_i\| \quad \|R_i^B\|_F = r(h_B, h_i) \|\mathbf{u}_B\| \|\mathbf{v}_i\|. \quad (20)$$

Step 3: The following auxiliary lemma provides a bound on $\|\mathbf{u}_A\|$ in terms of $|A|$ and the affinity lower bound δ .

Lemma 4.5. *Let A be equal to the terminal nodes of a clan in \mathcal{T} and let \mathbf{u}_A be the vector of Eq. (18). Then,*

$$\|\mathbf{u}_A\|^2 \geq \begin{cases} (2\delta^2)^{\log|A|} & \delta^2 \leq 0.5, \\ 2\delta^2 & \delta^2 > 0.5. \end{cases} \quad (21)$$

Similar bounds hold for $\|\mathbf{u}_B\|^2$ and $\|\mathbf{v}_k\|^2$. Having described steps 1-3, we are now ready to conclude the proof of Theorem 4.1. To this end, we use the following auxiliary lemma, which follows from steps 1 and 2.

Lemma 4.6. *Let $C = A \cup B$, where A and B are non-adjacent subsets of terminal nodes, that each forms a clan in \mathcal{T} . Then*

$$\begin{aligned} \sigma_2(R_C)^2 &\geq \frac{1}{4} \min\{\|\mathbf{u}_A\|, \|\mathbf{u}_B\|\}^2 \times \\ &\quad \min_j \min_{k \neq j} \|\mathbf{v}_k\|^2 (1 - r(h_j, h_k))^2 \min\{\max_k r(h_A, h_k), \max_k r(h_B, h_k)\}^2. \end{aligned} \quad (22)$$

Next, we insert the lower bounds in Eqs. (2) and (21) into Eq. (22). For $\delta^2 > 0.5$,

$$\sigma_2^2(R^C) \geq \frac{1}{4} (2\delta^2)(2\delta^2)\delta^2(1 - \xi^2)^2 = \delta^6(1 - \xi^2)^2.$$

For $\delta^2 \leq 0.5$ we obtain,

$$\sigma_2^2(R^C) \geq \frac{1}{4} (2\delta^2)^{\log|A| + \log|B|} \delta^2 (1 - \xi^2)^2 = \frac{1}{4} (2\delta^2)^{\log|A||B|} \delta^2 (1 - \xi^2)^2. \quad (23)$$

Since A, B are non adjacent subsets, there are at least two additional observed nodes that are not in $A \cup B$. It follows that $|A| + |B| \leq m - 2$ and hence $|A||B| < m^2/4$. Replacing $|A||B|$ with $m^2/4$ in (23) gives

$$\sigma_2^2(R^C) \geq \frac{1}{4} (2\delta^2)^{\log(m^2/4)} \delta^2 (1 - \xi^2)^2 = \frac{1}{4} (2\delta^2)^{2\log(m/2)} \delta^2 (1 - \xi^2)^2,$$

which completes the proof of Theorem 4.1. \square

4.2 Required number of samples for exact reconstruction

In this section, we focus on the finite sample setting, where we can only compute an approximate affinity matrix \hat{R} . For NJ, the finite sample setting was addressed in [2], where NJ was proved to reconstruct the correct tree if the estimated distance matrix \hat{D} satisfies Eq. (8). In the following lemma we derive an analogue result for SNJ.

Lemma 4.7. *Assume that Eq. (2) holds. Then a sufficient condition for spectral neighbor joining to recover the correct tree from \hat{R} is that*

$$\|R - \hat{R}\| \leq \begin{cases} \frac{f(m, \delta, \xi)}{2} & \delta^2 \leq 0.5 \\ \frac{1}{2} \delta^3 (1 - \xi^2) & \delta^2 > 0.5. \end{cases} \quad (24)$$

Next, we derive a concentration bound on the similarity matrix. This yields an upper bound on the number of samples required to obtain an estimated similarity matrix that satisfies Eq. (24). For simplicity, the finite sample bound is derived for the Jukes Cantor (JC) model, a popular model in phylogenetic inference,

see [13]. In the JC model, we assume that the probability over the d states in all the nodes is uniform, and that the stochastic matrix between adjacent nodes h_i, h_j is equal to

$$\Pr(h_i|h_j)_{kl} = \begin{cases} 1 - \theta(i, j) & k = l \\ \theta(i, j)/(d - 1) & \text{otherwise,} \end{cases}$$

where $\theta(i, j)$ is the mutation rate between nodes h_i and h_j . Under these assumptions, the affinity between terminal nodes in Eq. (4) simplifies to

$$R(i, j) = \left(1 - \frac{d}{d-1}\theta(i, j)\right)^{d-1}.$$

By assumption (2) $R(i, j) \geq \delta > 0$, and hence $\theta(i, j) < (d - 1)/d$. Given n i.i.d. realizations $\{x^l\}_{l=1}^n$ from the Jukes-Cantor model, we estimate $\hat{\theta}$ and \hat{R} via

$$\hat{\theta}(i, j) = \min \left\{ \frac{1}{n} \sum_{l=1}^n \mathbf{1}_{x_i^l \neq x_j^l}, \frac{d-1}{d} \right\} \quad \hat{R}(i, j) = \left(1 - \frac{d}{d-1}\hat{\theta}(i, j)\right)^{d-1}. \quad (25)$$

Applying SNJ to \hat{R} estimated via Eq. (25), we have the following guarantee.

Theorem 4.2. *Assume the data was generated according to the Jukes-Cantor model. If the number of samples n satisfies*

$$n \geq \begin{cases} \frac{2d^2m^2}{f(m, \delta, \xi)^2} \log \left(\frac{2m^2}{\varepsilon} \right) & \delta^2 \leq 0.5 \\ \frac{2d^2m^2}{\delta^6(1-\xi^2)^2} \log \left(\frac{2m^2}{\varepsilon} \right) & \delta^2 > 0.5, \end{cases}$$

where $f(m, \delta, \xi)$ was defined in (14), then SNJ will recover the correct tree topology with probability at least $1 - \varepsilon$.

To understand the dependency of n on the number of terminal nodes m , we replace $f(m, \delta, \xi)$ with its definition (14), and treat δ, ξ and d as constants. For $\delta^2 \leq 0.5$,

$$n = \Omega \left(m^{3-4\log_2 \delta} \log(m/\varepsilon) \right).$$

If $\delta^2 > 0.5$,

$$n = \Omega \left(m^2 \log(m/\varepsilon) \right).$$

Thus, up to a logarithmic factor, the number of samples required for an exact recovery of the tree is quadratic in m for $\delta^2 > 0.5$, but can reach $\Omega(m^\beta)$ with exponent $\beta \rightarrow \infty$ for very low values of δ . Next, considering the dependence on ξ , Theorem 4.2 implies that n scales as $\Omega(1/(1 - \xi^2))$. A high value of ξ corresponds to a tree that has at least one very short edge, and is thus hard to reconstruct. A similar result appears in the guarantee derived by Atteson in Eq. (8), which depends on the minimal distance between adjacent nodes. As we illustrate in Section 6 via simulations, the empirical performance of SNJ is in accordance to this theoretical analysis.

The proof of theorem 4.2 is based on the following auxiliary lemma, which states a concentration result on the estimated matrix \hat{R} .

Lemma 4.8. *Let $\hat{R} \in \mathbb{R}^{m \times m}$ be the matrix given by Eq. (25). Then*

$$\Pr \left(\|\hat{R} - R\|_2 \leq t \right) \geq 1 - 2m^2 \exp \left(- \frac{2mt^2}{d^2m^2} \right).$$

Proof of Theorem 4.2. We prove the finite sample theorem by combining Lemma 4.7 with the concentration bound on \hat{R} in Lemma 4.8. For $\delta^2 \leq 0.5$, we replace t with $f(m, \delta, \xi)/2$ in Lemma 4.8,

$$\Pr \left(\|\hat{R} - R\|_2 \leq \frac{f(m, \delta, \xi)}{2} \right) \geq 1 - 2m^2 \exp \left(- \frac{2n(f(m, \delta, \xi)/2)^2}{d^2 m^2} \right).$$

Let $1 - \varepsilon$ be a lower bound on this probability, such that

$$1 - 2m^2 \exp \left(- \frac{2n(f(m, \delta, \xi)/2)^2}{d^2 m^2} \right) \geq 1 - \varepsilon.$$

Rearranging the above equation yields the following lower bound on n in terms of m, d and ε ,

$$n \geq \frac{2d^2 m^2}{f(m, \delta, \xi)^2} \log \left(\frac{2m^2}{\varepsilon} \right),$$

which concludes the proof for $\delta^2 \leq 0.5$. For $\delta^2 > 0.5$, we replace $f(m, \delta, \xi)$ with $\delta^3(1 - \xi^2)$. \square

5 Comparison between Atteson's NJ guarantee and its SNJ analogue

In this section we assume a simple model of a perfect binary tree, where the affinity between all adjacent nodes is equal to δ . For this model we make an explicit comparison between the NJ sufficient condition (8) for perfect tree recovery and its SNJ analogue Lemma 4.7. The main insight is that for various regimes of the affinity δ and number of taxa m , obtaining an accurate tree estimate requires a smaller number of samples for SNJ, compared to NJ. The comparison between the methods is done by the following three steps:

1. In Eq. (28) we derive a bound on the accuracy of \hat{R} that is *less strict* than the NJ bound in (8). In other words, Eq. (8) implies Eq. (28).
2. In Eq. (31) we derive a bound on the accuracy of \hat{R} that is *stricter* than the SNJ guarantee in Lemma (4.7). That is, Eq. (31) implies Lemma 4.7.
3. Comparing (28) and (31) we show that the NJ guarantee is *stricter* than its NJ analogue in the regimes of low δ or a large number of taxa.

Step 1: Under the assumption that the similarity between all adjacent nodes is δ , the NJ sufficient condition (8) simplifies to

$$|\log \hat{R}(i, j) - \log R(i, j)| = \left| \log \frac{\hat{R}(i, j)}{R(i, j)} \right| \leq -\frac{\log \delta}{2} = \delta^{-0.5} \quad \forall i, j.$$

Taking an exponent on both sides we obtain

$$\delta^{0.5} R(i, j) < \hat{R}(i, j) < \delta^{-0.5} R(i, j) \quad \forall i, j.$$

Multiplying by -1 and adding $R(i, j)$ we get

$$(1 - \delta^{-0.5})R(i, j) < R(i, j) - \hat{R}(i, j) < (1 - \delta^{0.5})R(i, j) \quad \forall i, j. \quad (26)$$

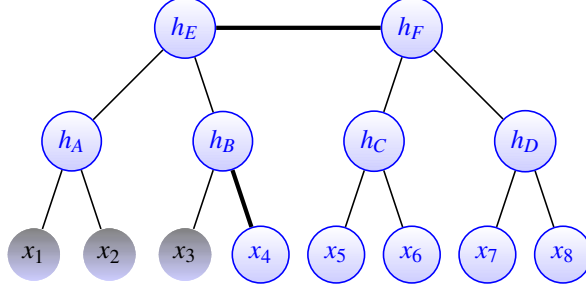


Figure 6: A perfect binary tree model with $m = 8$ terminal nodes. For proof of Lemma 3.2, the terminal nodes in A are colored in darker shade of gray. The thick edges form the minimal set that separate A from A^c . The quartet $i = 1, k = 3, j = 4$ and $l = 5$ satisfy $i, k \in A, j, l \in A^c$ but their topology is not as in Figure 2.

Since $0 < \delta < 1$, if Eq. (26) holds, then

$$|R(i, j) - \hat{R}(i, j)| \leq \delta^{-0.5} R(i, j) \quad \forall i, j. \quad (27)$$

Let A, B, C and D be four subsets of terminal nodes that correspond to four clans of \mathcal{T} , such that the pairs (A, B) and (C, D) are adjacent subsets, see Figure 6. For a perfect binary model, the affinity between all pairs $i \in A \cup B$ and $j \in C \cup D$ is equal to $\delta^{2 \log_2(m)-1}$, and hence Eq. (27) implies

$$|R(i, j) - \hat{R}(i, j)| \leq \delta^{2 \log_2(m)-1.5} \quad \forall i \in A \cup B, j \in C \cup D. \quad (28)$$

Concluding the derivation of step 1, for a perfect binary tree model, Eq. (28) is a necessary condition for Eq. (8) to hold.

Step 2: For the SNJ guarantee, the inequality $\|R - \hat{R}\|_2 \leq \sqrt{m} \|R - \hat{R}\|_\infty$ implies that if

$$\|R - \hat{R}\|_\infty \leq \begin{cases} \frac{1}{2\sqrt{m}} f(m, \delta, \xi) & \delta^2 \leq 0.5 \\ \frac{1}{2\sqrt{m}} \delta^3 (1 - \xi^2) & \delta^2 > 0.5, \end{cases} \quad (29)$$

then the conditions of Lemma 4.7 hold. For $\delta^2 \leq 0.5$, replacing $f(m, \delta, \xi)$ with its definition in Eq. (14) yields

$$\|R - \hat{R}\|_\infty \leq \frac{1}{4\sqrt{m}} (2\delta^2)^{\log_2(m)-1} \delta (1 - \xi^2) = \frac{\sqrt{m}}{8} (\delta^2)^{\log_2(m)} \delta^{-1} (1 - \xi^2). \quad (30)$$

Concluding the derivation of this step, SNJ will recover the exact tree if

$$\|R - \hat{R}\|_\infty \leq \begin{cases} \frac{\sqrt{m}}{8} (\delta^2)^{\log_2(m)} \delta^{-1} (1 - \xi^2) & \delta^2 \leq 0.5 \\ \frac{1}{2\sqrt{m}} \delta^3 (1 - \xi^2) & \delta^2 > 0.5. \end{cases} \quad (31)$$

Step 3: For $\delta^2 \leq 0.5$, the bound in Eq. (28) is tighter by a factor of $1/\sqrt{m}$ compared to Eq. (31). Hence the accuracy condition on \hat{R} is less strict for SNJ compared to NJ. This advantage increases for trees with a large number of terminal nodes m . For $\delta^2 > 0.5$, the bound in Eq. (29) is $O(m^{-0.5})$, while the bound in (28) is $O(m^{\log_2(\delta^2)})$. This implies that both bounds are of the same order when $\log_2(\delta^2) = -0.5$, or $\delta \approx 0.84$. Figure 7 compares the performance of NJ and SNJ over perfect binary trees with $m = 512$ nodes for four values of δ that satisfy $\delta^2 > 0.5$. As expected from our analysis, the advantage of SNJ is larger at lower values of δ . In this experiment, the two methods achieve similar accuracy for $\delta \approx 0.9$.

5.1 The spectral criterion and quartet based inference

Quartet based inference is a popular approach to recover latent tree models, see for example [37, 1, 35] and references therein. Since for a tree with m terminal nodes there are $O(m^4)$ quartets, these methods are often characterized by two steps: (i) estimating the topology for a large number of randomly sampled quartets of terminal nodes. (ii) Finding the tree that is consistent with the topology of the largest number of quartets, as estimated in step (i). The drawback of this approach is that in general, the second step poses a computationally hard problem, see [8].

Mihaescu et. al. [29] derived a link between quartet methods and NJ by proving a new guarantee for NJ. Loosely speaking, NJ will recover the correct tree if the estimated distance matrix is *consistent* with the topology of all possible quartets in the tree. Denote by $w(i, j; k, l)$ the value of the following 2×2 determinant,

$$w(i, j; k, l) = \begin{vmatrix} R(i, k) & R(i, l) \\ R(j, k) & R(j, l) \end{vmatrix},$$

where $(i, j; k, l)$ represent the quartet of terminal nodes x_i, x_j, x_k and x_l . Consider a subtree that contains, as terminal nodes, the quartet x_i, x_j, x_k and x_l . By Lemma 3.1 $w(i, j; k, l) = 0$ if and only if the pairs (x_i, x_j) and (x_k, x_l) are siblings. Thus, one can use the value of $w(i, j; k, l)$ to determine the topology of a quartet. Based on this property, several works derived quartet based methods. Anandkumar et. al. [1] developed recursive least grouping, which merges nodes i, j if the estimated values $\hat{w}(i, j; k, l)$ satisfy

$$\hat{w}(i, j; k, l) < t \quad \forall k, l.$$

for some threshold t . To reconstruct a three layer tree, [20] applied spectral clustering to the following score matrix,

$$S(i, j) = \sum_{k, l} w(i, j; k, l).$$

Here, we derive a link between spectral neighbor joining and the quartet approach. Let A and B be two subsets of terminal nodes that are equal to the observed nodes of two clans in a tree, and let $C = A \cup B$. Combining Eq. (35) with Lemma 4.4 gives

$$\sigma_2(R^C)^2 = \frac{\sum_{j, k} (\|R_j^A\|_F \|R_k^B\|_F - \|R_j^B\|_F \|R_k^A\|_F)^2}{2\sigma_1(R^C)^2}. \quad (32)$$

The link between SNJ and quartet methods is set by the following lemma.

Lemma 5.1. *The numerator in Eq. (32) is equal to*

$$\sum_{j, k} (\|R_j^A\|_F \|R_k^B\|_F - \|R_j^B\|_F \|R_k^A\|_F)^2 = \frac{1}{2} \sum_{i_1, i_2 \in A \cup B} \sum_{l_1, l_2 \notin A \cup B} w(i_1, i_2; l_1, l_2).$$

Lemma 5.1 sheds new light on the spectral neighbor joining criterion for merging subsets of terminal nodes. At each iteration, SNJ merges two subsets A, B that minimize the following *weighted quartet score*,

$$\sigma_2(R^C)^2 = \frac{1}{\sigma_1(R^C)^2} \sum_{i, j \in A \cup B} \sum_{k, l \in (A \cup B)^c} w(i, j; k, l)^2,$$

where $w(i, j; k, l)^2$ serves as a measure of consistency between the quartet i, j, k, l and the potential merge of $A \cup B$. Thus, similar to the idea behind quartet methods, the result of each step is a merge that maximizes the consistency across all possible quartets $i, j \in A \cup B$ and $k, l \in (A \cup B)^c$.

6 Simulation results

We compare the performance of SNJ vs. NJ for three types of trees: (i) perfect binary trees with equal similarity between all adjacent nodes. (ii) Caterpillar trees, where the non terminal nodes form a path graph, and (iii) Trees constructed according to Kingman’s coalescence model [52], a common phylogenetic model. In all three cases the transition matrices between adjacent nodes follow the Jukes Cantor model. The code for SNJ and scripts to reproduce our results can be found at <https://github.com/NoahAmsel/spectral-tree-inference>. All simulations were done with the Python phylogenetic computing library Dendropy [49].

The accuracy of a recovered tree is evaluated by the Robinson-Foulds (RF) distance [11], a popular measure for comparison between trees. The RF distance between two trees \mathcal{T}_1 and \mathcal{T}_2 counts the number of partitions in \mathcal{T}_1 that are not present in \mathcal{T}_2 and the number of partitions in \mathcal{T}_2 not present in \mathcal{T}_1 .

Figure 7 shows, for a perfect binary tree with $m = 512$ terminal nodes, the RF distance between the tree and its NJ and SNJ estimations, as a function of the sequence length n , for four values of $\delta = 0.75, 0.8, 0.85, 0.9$. The results are averaged over 10 realizations of the tree model. As expected from the theoretical analysis in Section 5, the advantage of SNJ over NJ increases for trees with high mutation rates.

Next, we consider caterpillar trees. In general, these trees are more challenging to recover than balanced ones, as shown in [26]. In our simulation, the similarity between all pairs of adjacent nodes was equal to $\delta = 0.92$, and the sequence length was $n = 2000$. Figure 8 shows the value of $\log(1 + RF)$, as a function of the number of leaves m . Both methods successfully recovered the tree for $m = 100$ leaves. However, the advantage of SNJ over NJ becomes apparent for larger trees. This experiment is consistent with the theoretical analysis of section 5.

For the third simulation, we generated trees with $m = 256$ leaves according to Kingman’s coalescent model. The similarity between two adjacent nodes h_A, h_B is equal to δ^l , where l is the edge length of $e(h_A, h_B)$. Figure 8 (right) shows the accuracy of the recovered tree as a function of δ . Note that with only $n = 2000$ samples, both methods don’t achieve an exact recovery of the tree. The reason is that trees generated according to the coalescent model have relatively short edges at the bottom layers of the tree. In contrast to NJ, the performance of SNJ is stable for all values of δ .

Acknowledgements Y.K. acknowledges support by NIH grants R01HG008383, R01GM131642, and 2P50CA121974. BN is incumbent of the William Petschek professorial chair of mathematics. Part of this work was done while BN was on sabbatical at the Institute for Advanced Study at Princeton. He gratefully acknowledges the support from the Charles Simonyi Endowment. The authors would like to thank Junhyong Kim, Stefan Steinerberger, Yariv Aizenbud and Ronald Coifman for their help in various aspects of the paper.

A Proof of Lemma 3.2

Proof. First, we assume that the subset A forms the terminal nodes of a clan. Hence, there is a single edge in the tree such that all paths between $\{x_i\}_{i \in A}$ and $\{x_i\}_{i \in A^c}$ pass through it. We denote this edge by $e(h_A, h_B)$. Let $i, k \in A$ and $j, l \in A^c$. Then all paths $i \rightarrow j, i \rightarrow l, k \rightarrow j$ and $k \rightarrow l$ pass through the common edge $e(h_A, h_B)$. It follows that the topology of the quartet is as in Figure 2.

For the other direction, assume that all quartets x_i, x_j, x_k, x_l , where $(i, k) \in A$ and $(j, l) \in A^c$ have a topology as in Figure 2. By way of contradiction, assume that A is *not equal* to the terminal nodes of a clan. Consider a set of edges in the tree such that all paths between A from A^c pass through at least one of the edges in the set. If A is not a clan, there is no unique edge in the tree such that all paths between A and A^c pass through it, and hence any such set must contain at least two edges, which we denote by $e(h_1, h_2)$ and

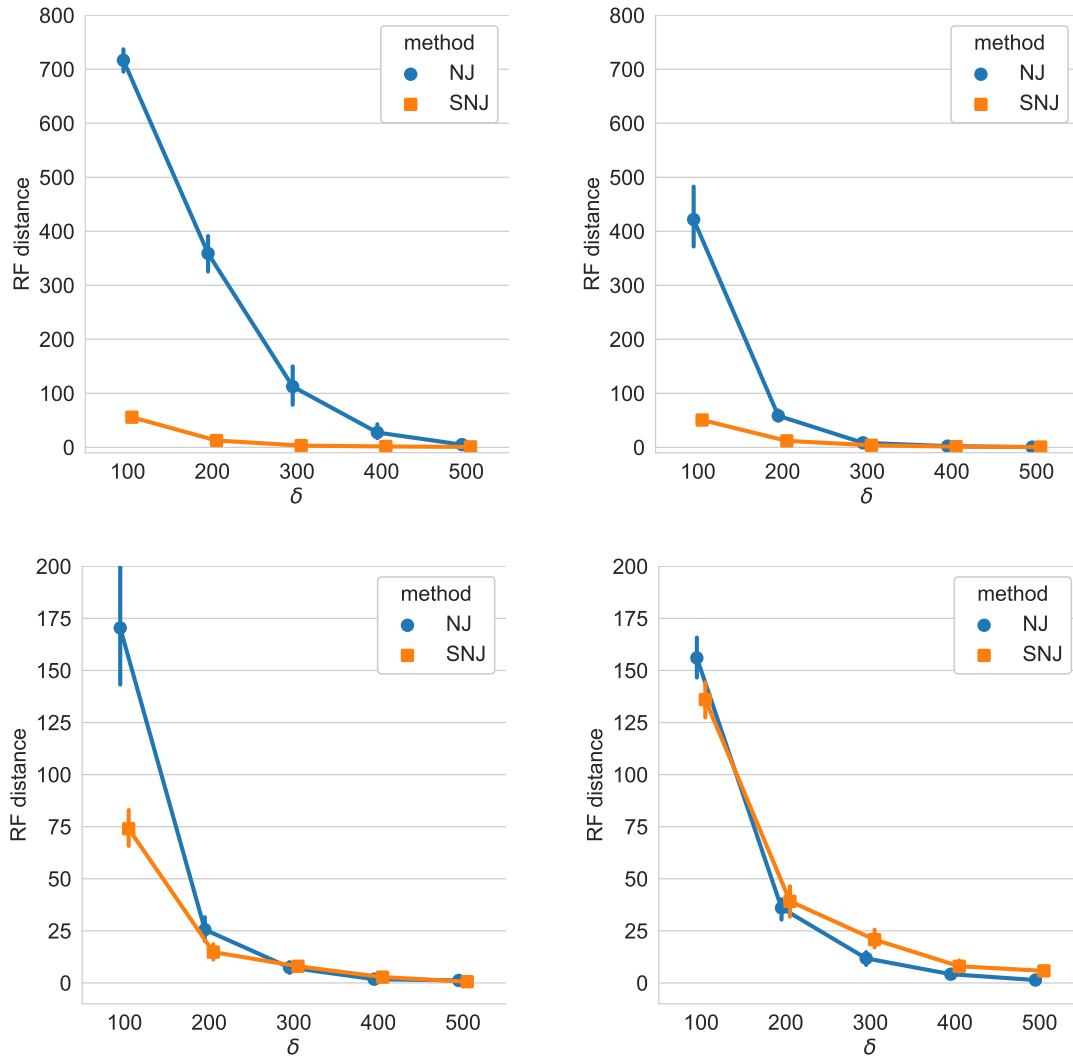


Figure 7: Comparison between NJ and SNJ for perfect binary trees with $m = 512$ nodes, and four value of δ . The advantage of SNJ over NJ increases as δ decreases.

$e(h_3, h_4)$. Note that these edges might connect between two non terminal nodes, or between one terminal and one non terminal node, see illustration in Figure 6. Assume w.l.o.g. that h_1 is closer to nodes in A than h_2 and that h_3 is closer to A than h_4 . We pick a quartet of nodes x_i, x_j, x_k, x_l in the following way: x_i is chosen such that $i \in A$ and is closest to h_1 among h_1, h_2, h_3 and h_4 . Similarly, x_k, x_j, x_l are chosen such that $k \in A$ and $j, l \in A^c$ and they are closest to h_3, h_2, h_4 respectively. The topology of this quartet is not as in Figure 2, which contradicts our assumption. Thus, A must equal the terminal nodes of a clan. \square

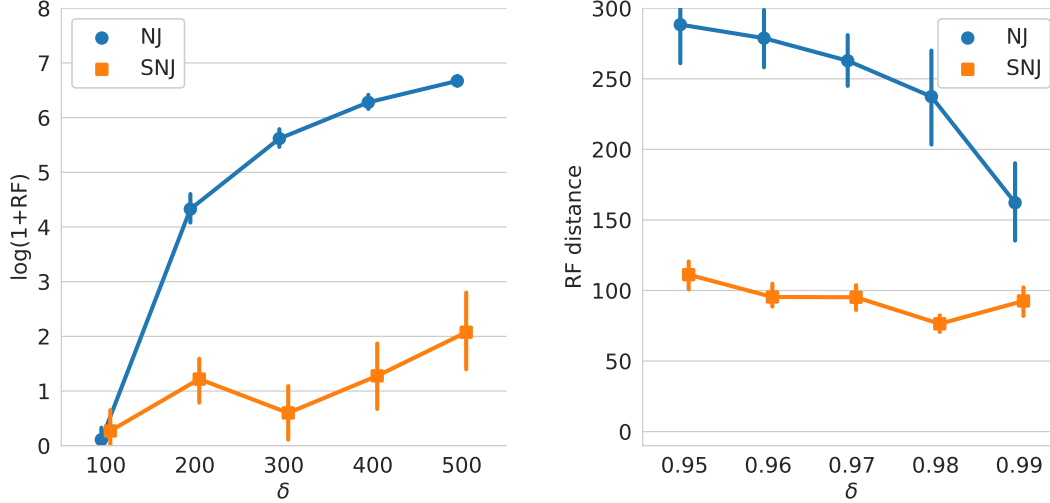


Figure 8: Left: the accuracy of NJ and SNJ in recovering caterpillar trees with all edges having the same parameter $\delta = 0.92$, and with varying number of leaves. Right: the accuracy of NJ and SNJ for trees generated by Kingman’s coalescent model, with varying mutation rates.

B Proofs of lemmas of Section 4

We first present the following auxiliary lemma.

Lemma B.1. *Let R_j^A and R_k^A be two different blocks of the matrix R^C given in Eq. (15). Then,*

$$\|(R_k^A)^T R_j^A\|_F = \|R_k^A\|_F \|R_j^A\|_F.$$

Similarly, with R_j^B and R_k^B also two blocks of R^C corresponding to the subtree B ,

$$\|(R_k^A)^T R_j^A (R_j^B)^T R_k^B\|_F = \|R_j^A\|_F \|R_k^A\|_F \|R_j^B\|_F \|R_k^B\|_F.$$

Proof of Lemma B.1. By Eq. (19), R_j^A and R_k^A are rank one matrices, with the *same* left singular vector \mathbf{u}_A . Thus,

$$\begin{aligned} \|(R_k^A)^T R_j^A\|_F &= \|\mathbf{v}_k r(h_A, h_k) \mathbf{u}_A^T \mathbf{u}_A r(h_A, h_j) \mathbf{v}_j^T\|_F \\ &= \|\mathbf{u}_A\|^2 r(h_A, h_j) r(h_A, h_k) \|\mathbf{v}_k \mathbf{v}_j^T\|_F \\ &= \|\mathbf{u}_A\|^2 \|\mathbf{v}_j\| \|\mathbf{v}_k\| r(h_A, h_j) r(h_A, h_k) = \|R_j^A\|_F \|R_k^A\|_F. \end{aligned}$$

Similarly,

$$(R_k^A)^T R_j^A (R_j^B)^T R_k^B = \mathbf{v}_k r(h_A, h_k) \mathbf{u}_A^T \mathbf{u}_A r(h_A, h_j) \mathbf{v}_j^T \mathbf{v}_j r(h_B, h_k) \mathbf{u}_B^T \mathbf{u}_B r(h_B, h_j) \mathbf{v}_j^T.$$

Taking the Frobenius norm yields the second equation of the lemma. \square

Proof of Lemma 4.1. Consider a perfect binary tree, as in Figure 6. The affinity between all adjacent nodes is δ , except the edge that splits the tree into two subsets of size $m/2$, whose affinity is ξ . We assume that the four clans attached to h_A, h_B, h_C and h_D were correctly reconstructed during the first iterations of the algorithm. The last step to reconstruct the tree is to estimate the inner topology of h_A, h_B, h_C and h_D . The paths between terminal nodes in $A \cup B$ and $C \cup D$ contain $2 \log_2(m/2)$ edges with affinity δ and a single edge with affinity ξ . In contrast, paths connecting terminal nodes in A and terminal nodes in B are shorter, with only $2 \log_2(m/2)$ edges with affinity δ . A similar property holds for paths connecting terminal nodes in C to terminal nodes in D . Consider the matrix $R^{A \cup C}$ of size $m/2 \times m/2$, that contains the affinities between nodes in $A \cup C$ and $B \cup D$. This matrix has the following block structure,

$$R^{A \cup C} = \delta^{2 \log_2(m/2)} \begin{bmatrix} \mathbf{1}\mathbf{1}^T & \xi \mathbf{1}\mathbf{1}^T \\ \xi \mathbf{1}\mathbf{1}^T & \mathbf{1}\mathbf{1}^T \end{bmatrix},$$

where $\mathbf{1}$ is a vector of ones of length $m/4$. The second eigenvalue of $R^{A \cup C}$ is equal to

$$\sigma_2(R^{A \cup C}) = \frac{m}{4} \delta^{2 \log_2(m/2)} (1 - \xi) = \frac{1}{2} (2\delta^2)^{\log_2(m/2)} (1 - \xi) = \frac{f(m, \delta, \xi)}{\delta(1 + \xi)}, \quad (33)$$

which concludes the proof for $\delta^2 \leq 0.5$. For $\delta^2 > 0.5$, consider a tree with 4 terminal nodes. Inserting $m = 4$ in (33) we obtain

$$\sigma_2(R^{A \cup C}) = \delta^2 (1 - \xi),$$

which concludes the proof for $\delta^2 > 0.5$. □

Proof of Lemma 4.3. Denote the largest singular value of M by σ_1 . Then,

$$\|M\|_F^2 = \sigma_1^2 + \sigma_2^2, \quad \|M^T M\|_F^2 = \sigma_1^4 + \sigma_2^4, \quad (34)$$

where we used the fact that the singular values of $M^T M$ are equal to the square of the singular values of M . The numerator in Eq. (16) is thus equal to

$$\|M\|_F^4 - \|M^T M\|_F^2 = (\sigma_1^2 + \sigma_2^2)^2 - (\sigma_1^4 + \sigma_2^4) = 2\sigma_1^2 \sigma_2^2. \quad (35)$$

Since $0 \leq \sigma_2 \leq \sigma_1$,

$$\sigma_2^2 \geq \frac{1}{2} \frac{2\sigma_1^2 \sigma_2^2}{\sigma_1^2 + \sigma_2^2}. \quad (36)$$

Combining (34), (35) and (36) proves Eq. (16). □

Proof of Lemma 4.4. Recall that the matrix R^C has a block form given in Eq. (15). Thus,

$$\|R^C\|_F^2 = \sum_{j=1}^l (\|R_j^A\|_F^2 + \|R_j^B\|_F^2) \quad (37)$$

and

$$\|R^C\|_F^4 = \sum_{j,k=1}^l \|R_j^A\|_F^2 \|R_k^A\|_F^2 + \|R_j^A\|_F^2 \|R_k^B\|_F^2 + \|R_j^B\|_F^2 \|R_k^A\|_F^2 + \|R_j^B\|_F^2 \|R_k^B\|_F^2. \quad (38)$$

To compute $\|(R^C)^T R^C\|_F^2$, by Eq. (15),

$$(R^C)^T R^C = \begin{bmatrix} R_1^T \\ R_2^T \\ \vdots \\ R_l^T \end{bmatrix} [R_1 \quad R_2 \quad \dots \quad R_l] = \begin{bmatrix} R_1^T R_1 & R_1^T R_2 & \dots & R_1^T R_l \\ R_2^T R_1 & R_2^T R_2 & \dots & R_2^T R_l \\ \vdots & \vdots & \ddots & \vdots \\ R_l^T R_1 & R_l^T R_2 & \dots & R_l^T R_l \end{bmatrix},$$

where R_i was defined as the concatenation of R_i^A and R_i^B . Thus,

$$\begin{aligned} \|(R^C)^T R^C\|_F^2 &= \sum_{j,k=1}^l \|R_j^T R_k\|_F^2 = \sum_{j,k=1}^l \|(R_j^A)^T R_k^A + (R_j^B)^T R_k^B\|_F^2 \\ &= \sum_{j,k=1}^l \left(\|(R_j^A)^T R_k^A\|_F^2 + \|(R_j^B)^T R_k^B\|_F^2 + 2\|(R_j^A)^T R_k^A (R_j^B)^T R_k^B\|_F^2 \right). \end{aligned} \quad (39)$$

Applying Lemma B.1 to the various terms in Eq. (39) gives

$$\|(R^C)^T R^C\|_F^2 = \sum_{j,k=1}^l \|R_j^A\|_F^2 \|R_k^A\|_F^2 + \|R_j^B\|_F^2 \|R_k^B\|_F^2 + 2\|R_j^A\|_F \|R_k^A\|_F \|R_j^B\|_F \|R_k^B\|_F.$$

Combining the above equation and (38) yields

$$\begin{aligned} \|R^C\|_F^4 - \|(R^C)^T R^C\|_F^2 &= \sum_{j,k=1}^l \left(\|R_j^A\|_F^2 \|R_k^B\|_F^2 + \|R_k^A\|_F^2 \|R_j^B\|_F^2 \right. \\ &\quad \left. - 2\|R_j^A\|_F \|R_k^A\|_F \|R_j^B\|_F \|R_k^B\|_F \right) \\ &= \sum_{j,k=1}^l \left(\|R_j^A\|_F \|R_k^B\|_F - \|R_k^A\|_F \|R_j^B\|_F \right)^2. \end{aligned}$$

□

Proof of Lemma 4.5. Let \mathcal{T}_A be a clan of the tree \mathcal{T} that contains $|A|$ terminal nodes and let h_A be the root of the clan. We say that a terminal node x_i is of depth k if the path between x_i and h_A contains exactly k edges. Let \mathbf{u}_A be the vector of affinities between the terminal nodes of \mathcal{T}_A and its root h_A . Given the multiplicative property of the affinity function along the paths as discussed in Section 3.1 and assumption (2), $\|\mathbf{u}_A\|$ is clearly at least as large as its norm if we assume all edge affinities are exactly δ .

Next, considering all possible trees with $|A|$ terminal nodes, we show that if $\delta^2 \leq 0.5$, the norm $\|\mathbf{u}\|$ is minimal for a perfect binary tree. In contrast, if $\delta^2 > 0.5$, the norm is minimized for a caterpillar tree. For both cases, our proof is based on altering the tree \mathcal{T}_A by removing a pair of adjacent terminal nodes x_1, x_2 of depth j , and attaching them to a terminal node x_i of depth k . We denote by \mathbf{u}_2 the vector of affinities between the terminal nodes and h in the altered tree. The difference between $\|\mathbf{u}_1\|^2$ and $\|\mathbf{u}_2\|^2$ is equal to

$$\|\mathbf{u}_2\|^2 - \|\mathbf{u}_1\|^2 = 2\delta^{2(k+1)} - 2\delta^{2j} + \delta^{2(j-1)} - \delta^{2k}. \quad (40)$$

The first two terms are due to the shift of x_1, x_2 from depth j to depth $k+1$. The last two terms are due to the non terminal node attached to x_1, x_2 becoming terminal, while x_i becoming non terminal. We can rewrite Eq. (40) as

$$\|\mathbf{u}_2\|^2 - \|\mathbf{u}_1\|^2 = (\delta^2)^{j-1}(1 - 2\delta^2) - (\delta^2)^k(1 - 2\delta^2) = (1 - 2\delta^2)((\delta^2)^{j-1} - (\delta^2)^k). \quad (41)$$

For $\delta^2 < 0.5$, the above expression is negative if $j - 1 > k$. We can thus decrease the norm of the affinity vector by shifting pairs of adjacent terminal nodes of depth j to depth $k + 1$ where $k + 1 < j$. Repeating this step will decrease the norm up to a point where such a change is no longer possible. The extreme case is when the depth of all terminal nodes is equal to $\log_2(|A|)$. In this case, the norm of \mathbf{u} is equal to,

$$\|\mathbf{u}\|^2 = |A|\delta^{2\log_2(|A|)} = (2\delta^2)^{\log_2(|A|)}.$$

For $\delta^2 > 0.5$, Eq. (41) is negative if $k + 1 < j$. We can thus decrease the vector norm by increasing the depth of x_1, x_2 . Repeating this step will decrease the norm up to a point where the tree contains exactly one terminal node of depth i for $i = 1, \dots, |A| - 2$, and 2 terminal nodes of depth $|A| - 1$. The squared norm of the affinity vector is bounded by

$$\begin{aligned} \|\mathbf{u}_A\|^2 &= \sum_{i=1}^{|A|-1} \delta^{2i} + \delta^{2(|A|-1)} = \delta^2 \left(\sum_{i=0}^{|A|-2} \delta^{2i} + \delta^{2(|A|-2)} \right) \\ &\geq \delta^2 \left(\sum_{i=0}^{|A|-2} (0.5)^i + 0.5^{|A|-2} \right) = 2\delta^2, \end{aligned}$$

which concludes the proof. \square

Proof of Lemma 4.6. Combining Lemmas 4.3 and 4.4 with Eq. (37) gives

$$\sigma_2(\mathbf{R}^C)^2 \geq \frac{1}{2} \frac{\sum_{j,k=1}^l (\|\mathbf{R}_j^A\|_F \|\mathbf{R}_k^B\|_F - \|\mathbf{R}_j^B\|_F \|\mathbf{R}_k^A\|_F)^2}{\sum_{j=1}^l \|\mathbf{R}_j^A\|_F^2 + \|\mathbf{R}_j^B\|_F^2}. \quad (42)$$

Inserting Eq. (20) into Eq. (42) yields,

$$\begin{aligned} \sigma_2(\mathbf{R}^C)^2 &\geq \frac{1}{2} \|\mathbf{u}_A\|^2 \|\mathbf{u}_B\|^2 \times \\ &\quad \frac{\sum_{j,k=1}^l \left(\|\mathbf{v}_j\|^2 \|\mathbf{v}_k\|^2 (r(h_A, h_j)r(h_B, h_k) - r(h_A, h_k)r(h_B, h_j))^2 \right)}{\sum_{j=1}^l \left(\|\mathbf{u}_A\|^2 \|\mathbf{v}_j\|^2 r(h_A, h_j)^2 + \|\mathbf{u}_B\|^2 \|\mathbf{v}_j\|^2 r(h_B, h_j)^2 \right)}. \end{aligned} \quad (43)$$

We bound the ratio of sums in Eq. (43) by the minimum over individual ratios,

$$\begin{aligned} \sigma_2(\mathbf{R}^C)^2 &\geq \frac{1}{2} \|\mathbf{u}_A\|^2 \|\mathbf{u}_B\|^2 \times \\ &\quad \min_j \frac{\|\mathbf{v}_j\|^2 \sum_{k=1}^l \left(\|\mathbf{v}_k\|^2 (r(h_A, h_j)r(h_B, h_k) - r(h_A, h_k)r(h_B, h_j))^2 \right)}{\|\mathbf{u}_A\|^2 \|\mathbf{v}_j\|^2 r(h_A, h_j)^2 + \|\mathbf{u}_B\|^2 \|\mathbf{v}_j\|^2 r(h_B, h_j)^2}. \\ &= \frac{1}{2} \|\mathbf{u}_A\|^2 \|\mathbf{u}_B\|^2 \min_j \frac{\sum_{k=1}^l \left(\|\mathbf{v}_k\|^2 (r(h_A, h_j)r(h_B, h_k) - r(h_A, h_k)r(h_B, h_j))^2 \right)}{\|\mathbf{u}_A\|^2 r(h_A, h_j)^2 + \|\mathbf{u}_B\|^2 r(h_B, h_j)^2}. \end{aligned} \quad (44)$$

Let us focus on the term

$$r(h_A, h_j)r(h_B, h_k) - r(h_A, h_k)r(h_B, h_j).$$

Recall that h_j and h_k are nodes on the path from h_A to h_B . Obviously, if $k = j$ then this term vanishes. Else, if h_j is on the path traversing from h_A to h_k (i.e., the path is $h_A \rightarrow h_j \rightarrow h_k \rightarrow h_B$) the affinity multiplicative property implies

$$r(h_A, h_k) = r(h_A, h_j)r(h_j, h_k) \quad r(h_B, h_j) = r(h_B, h_k)r(h_k, h_j),$$

and hence

$$r(h_A, h_j)r(h_B, h_k) - r(h_A, h_k)r(h_B, h_j) = r(h_A, h_j)r(h_B, h_k)(1 - r(h_k, h_j)^2). \quad (45)$$

Similarly, if h_j is closer to h_B (i.e., the path is $h_A \rightarrow h_k \rightarrow h_j \rightarrow h_B$) then

$$r(h_A, h_j)r(h_B, h_k) - r(h_A, h_k)r(h_B, h_j) = r(h_A, h_k)r(h_B, h_j)(r(h_k, h_j)^2 - 1). \quad (46)$$

Combining Eq. (45) and Eq. (46),

$$\begin{aligned} & (r(h_A, h_j)r(h_B, h_k) - r(h_A, h_k)r(h_B, h_j))^2 = \\ & \max\{r(h_A, h_j)r(h_B, h_k), r(h_A, h_k)r(h_B, h_j)\}^2(1 - r(h_j, h_k)^2)^2. \end{aligned} \quad (47)$$

Inserting Eq. (47) into Eq. (44) we obtain,

$$\begin{aligned} \sigma_2(\mathcal{R}^C)^2 & \geq \frac{1}{2} \|\mathbf{u}_A\|^2 \|\mathbf{u}_B\|^2 \times \\ & \min_j \frac{\sum_{k=1}^l \|\mathbf{v}_k\|^2 \max\{r(h_A, h_j)r(h_B, h_k), r(h_A, h_k)r(h_B, h_j)\}^2(1 - r(h_j, h_k)^2)^2}{\|\mathbf{u}_A\|^2 r(h_A, h_j)^2 + \|\mathbf{u}_B\|^2 r(h_B, h_j)^2} \\ & \geq \frac{1}{2} \|\mathbf{u}_A\|^2 \|\mathbf{u}_B\|^2 \times \\ & \min_j \frac{\sum_{k=1}^l \|\mathbf{v}_k\|^2 \max\{r(h_A, h_j)r(h_B, h_k), r(h_A, h_k)r(h_B, h_j)\}^2(1 - r(h_j, h_k)^2)^2}{2 \max\{\|\mathbf{u}_A\| r(h_A, h_j), \|\mathbf{u}_B\| r(h_B, h_j)\}^2}. \end{aligned}$$

Note that for $k = j$ we have $r(h_j, h_k) = 1$. Next, we lower bound the sum over k by the maximal term $k \neq j$. Using the inequality for any non-negative elements $\max_k \{x_k y_k\} \geq \min_k \{x_k\} \max_k \{y_k\}$ yields

$$\begin{aligned} \sigma_2(\mathcal{R}^C)^2 & \geq \frac{1}{2} \|\mathbf{u}_A\|^2 \|\mathbf{u}_B\|^2 \times \\ & \min_j \min_{k \neq j} \|\mathbf{v}_k\|^2 (1 - r(h_j, h_k)^2)^2 \max_{k \neq j} \frac{\max\{r(h_A, h_j)r(h_B, h_k), r(h_A, h_k)r(h_B, h_j)\}^2}{2 \max\{\|\mathbf{u}_A\| r(h_A, h_j), \|\mathbf{u}_B\| r(h_B, h_j)\}^2}. \end{aligned} \quad (48)$$

For the numerator in (48), we apply the following inequality,

$$\max\{x_1 y_1, x_2 y_2\} \geq \max\{x_1, x_2\} \min\{y_1, y_2\}.$$

It follows that,

$$\begin{aligned} & \max_{k \neq j} \max\{r(h_A, h_j)r(h_B, h_k), r(h_A, h_k)r(h_B, h_j)\}^2 \\ & = \max\{\max_{k \neq j} r(h_B, h_k)r(h_A, h_j), \max_{k \neq j} r(h_A, h_k)r(h_B, h_j)\}^2 \\ & \geq \max\{r(h_A, h_j), r(h_B, h_j)\}^2 \min\{\max_{k \neq j} r(h_B, h_k), \max_{k \neq j} r(h_A, h_k)\}^2. \end{aligned} \quad (49)$$

For the denominator we have,

$$\max\{\|\mathbf{u}_A\|r(h_A, h_j), \|\mathbf{u}_B\|r(h_B, h_j)\}^2 \leq \max\{\|\mathbf{u}_A\|, \|\mathbf{u}_B\|\}^2 \max\{r(h_A, h_j), r(h_B, h_j)\}^2. \quad (50)$$

Inserting (49) and (50) into (48) we get

$$\sigma_2(R^C)^2 \geq \frac{1}{2} \|\mathbf{u}_A\|^2 \|\mathbf{u}_B\|^2 \times \min_j \min_{k \neq j} \|\mathbf{v}_k\|^2 (1 - r(h_j, h_k))^2 \frac{\min\{\max_{k \neq j} r(h_B, h_k), \max_{k \neq j} r(h_A, h_k)\}^2}{2 \max\{\|\mathbf{u}_A\|, \|\mathbf{u}_B\|\}^2}.$$

We conclude the proof by applying the equality $\frac{xy}{\max\{x, y\}} = \min\{x, y\}$,

$$\sigma_2(R^C)^2 \geq \frac{1}{4} \min\{\|\mathbf{u}_A\|, \|\mathbf{u}_B\|\}^2 \min_j \min_{k \neq j} \|\mathbf{v}_k\|^2 (1 - r(h_j, h_k))^2 \min\{\max_k r(h_A, h_k), \max_k r(h_B, h_k)\}^2.$$

□

Proof of Lemma 4.7. We prove the statement by induction. For simplicity, we assume $\delta^2 \geq 0.5$. A similar proof holds for $\delta^2 > 0.5$. Assuming that all pairs of subsets merged in the first k iterations were adjacent, we prove that the algorithm will merge another pair of adjacent subsets at step $k + 1$. In step 1, this assumption holds trivially, since no merges have taken place yet. Let A_i, A_j be a pair of adjacent subsets and let A_k, A_l be a pair of non-adjacent subsets. By our inductive assumption and Theorem 4.1,

$$\sigma_2(R^{A_i \cup A_j}) = 0, \quad \sigma_2(R^{A_k \cup A_l}) \geq f(m, \delta, \xi).$$

The Weyl inequality states that for any matrices A and B , $|\sigma_i(A + B) - \sigma_i(A)| \leq \|B\|$. Recall that \hat{R} is the estimate of the affinity matrix R . Letting $A = R^{A_i \cup A_j}$ and $B = \hat{R}^{A_i \cup A_j} - R^{A_i \cup A_j}$, Weyl's inequality implies

$$|\sigma_2(\hat{R}^{A_i \cup A_j}) - \sigma_2(R^{A_i \cup A_j})| \leq \|\hat{R}^{A_i \cup A_j} - R^{A_i \cup A_j}\|.$$

The spectral norm of a submatrix is bounded by the spectral norm of the full matrix, thus

$$|\sigma_2(\hat{R}^{A_i \cup A_j}) - \sigma_2(R^{A_i \cup A_j})| \leq \|\hat{R} - R\|.$$

For a pair of adjacent subsets (A_i, A_j) , since $\sigma_2(R^{A_i \cup A_j}) = 0$,

$$\sigma_2(\hat{R}^{A_i \cup A_j}) \leq \|\hat{R} - R\|.$$

For non-adjacent subsets (A_k, A_l) ,

$$\sigma_2(\hat{R}^{A_k \cup A_l}) \geq \sigma_2(R^{A_k \cup A_l}) - \|\hat{R} - R\| \geq f(m, \delta, \xi) - \|\hat{R} - R\|.$$

If $\|\hat{R} - R\| \leq \frac{f(m, \delta, \xi)}{2}$, then for any adjacent (A_i, A_j) and non adjacent (A_k, A_l)

$$\sigma_2(\hat{R}^{A_i \cup A_j}) \leq \sigma_2(\hat{R}^{A_k \cup A_l}). \quad (51)$$

Combining the merging criterion in (11) with Eq. (51) proves that SNJ will merge a pair of adjacent subsets in step $k + 1$. □

Proof of Lemma 4.8. Consider the estimates $\hat{\theta}(i, j)$ and $\hat{R}(i, j)$ in Eq. (25). Since $\hat{\theta}(i, j)$ is a sum of n Bernoulli random variables with success probability $\theta(i, j)$, then by Hoeffding's inequality,

$$\Pr\left(|\hat{\theta}(i, j) - \theta(i, j)| \geq t\right) \leq 2\exp(-2nt^2). \quad (52)$$

Define $g(\theta(i, j)) = (1 - \frac{d}{d-1}\theta(i, j))^{d-1}$ so that $\hat{R}(i, j) = g(\hat{\theta}(i, j))$. For $\theta(i, j) \in [0, 1]$ the function $g(\theta(i, j))$ is d -Lipschitz. Thus

$$|\hat{R}(i, j) - R(i, j)| = |g(\hat{\theta}(i, j)) - g(\theta(i, j))| \leq d|\hat{\theta}(i, j) - \theta(i, j)|. \quad (53)$$

Combining Eq. (53) with the tail bound in Eq. (52) we get,

$$\Pr\left(|\hat{R}(i, j) - R(i, j)| \geq t\right) = \Pr\left(|\hat{\theta}(i, j) - \theta(i, j)| \geq \frac{t}{d}\right) \leq 2\exp\left(-\frac{2nt^2}{d^2}\right).$$

Applying a union bound over all m^2 entries of $\hat{R} - R$ gives

$$\Pr\left(|\hat{R}(i, j) - R(i, j)| \leq t \quad \forall i, j\right) \geq 1 - 2m^2 \exp\left(-\frac{2nt^2}{d^2}\right).$$

Finally, since $\|\hat{R} - R\| \leq m \max_{i,j} |\hat{R}(i, j) - R(i, j)|$ then

$$\Pr\left(\|\hat{R} - R\| \leq t\right) \geq 1 - 2m^2 \exp\left(-\frac{2nt^2}{d^2 m^2}\right),$$

which concludes the proof. \square

C Proof of Lemma 5.1

We use the following two auxiliary lemmas. The first lemma, proven in [3], gives a general relation between the k size determinants of a square matrix and its singular values.

Lemma C.1. *We denote by $\{\sigma_i(S)\}$ the singular values of a square matrix $S \in \mathbb{R}^{m \times m}$. Let $\{A_i^k\}$ be all possible size k subsets of $1, \dots, m$ and let $S(A_i^k)$ be a submatrix of S that contains all elements S_{jl} where $j, l \in A_i^k$. Then*

$$\sum_i |S(A_i^k)| = \sum_i \prod_{j \in A_i^k} \sigma_j(S).$$

For subsets of size $k = 2$, lemma C.1 implies

$$\sum_{i_1, i_2} \begin{vmatrix} S(i_1, i_1) & S(i_1, i_2) \\ S(i_2, i_1) & S(i_2, i_2) \end{vmatrix} = \sum_{i \neq j} \sigma_i(S) \sigma_j(S).$$

The second lemma addresses the sum of all 2×2 determinants of an arbitrary matrix.

Lemma C.2. *Let $S = RR^T$ where R is a matrix of arbitrary size $d_1 \times d_2$. Then,*

$$\sum_{i_1, i_2} \sum_{l_1, l_2} \begin{vmatrix} R(i_1, l_1) & R(i_1, l_2) \\ R(i_2, l_1) & R(i_2, l_2) \end{vmatrix}^2 = 2 \sum_{i_1, i_2} \begin{vmatrix} S(i_1, i_1) & S(i_1, i_2) \\ S(i_2, i_1) & S(i_2, i_2) \end{vmatrix} \quad (54)$$

Proof of Lemma 5.1. Let $S = RR^T$. Combining Lemmas C.1 and C.2 gives

$$\sum_{i_1, i_2} \sum_{l_1, l_2} \begin{vmatrix} R(i_1, l_1) & R(i_1, l_2) \\ R(i_2, l_1) & R(i_2, l_2) \end{vmatrix}^2 = 2 \sum_{i \neq j} \sigma_i(S) \sigma_j(S) = 2 \sum_{i \neq j} (\sigma_i(R) \sigma_j(R))^2. \quad (55)$$

Let A and B be two clans in \mathcal{T} . Then according to Lemma 4.2, $\text{rank}(R^{A \cup B}) \leq 2$. Thus, by Eq. (55)

$$\sum_{i_1, i_2} \sum_{l_1, l_2} \begin{vmatrix} R^{A \cup B}(i_1, l_1) & R^{A \cup B}(i_1, l_2) \\ R^{A \cup B}(i_2, l_1) & R^{A \cup B}(i_2, l_2) \end{vmatrix}^2 = 4 \sigma_1(R^{A \cup B})^2 \sigma_2(R^{A \cup B})^2. \quad (56)$$

Combining Eq. (56) with Lemma 4.4 and Eq. (35) concludes the proof. \square

Proof of Lemma C.2. First, we expand the determinant:

$$\begin{aligned} \begin{vmatrix} R(i_1, l_1) & R(i_1, l_2) \\ R(i_2, l_1) & R(i_2, l_2) \end{vmatrix}^2 &= \left(R(i_1, l_1)R(i_2, l_2) - R(i_1, l_2)R(i_2, l_1) \right)^2 \\ &= R(i_1, l_1)^2 R(i_2, l_2)^2 - 2R(i_1, l_1)R(i_2, l_2)R(i_1, l_2)R(i_2, l_1) + R(i_1, l_2)^2 R(i_2, l_1)^2. \end{aligned}$$

Since $S = RR^T$ then $\sum_l R(i, l)^2 = S_{ii}$. Thus,

$$\sum_{l_1, l_2} R(i_1, l_1)^2 R(i_2, l_2)^2 = S(i_1, i_1)S(i_2, i_2).$$

Similarly,

$$\sum_{l_1, l_2} R(i_1, l_1)R(i_2, l_2)R(i_1, l_2)R(i_2, l_1) = \left(\sum_l R(i_1, l)R(i_2, l) \right)^2 = S(i_1, i_2)^2.$$

Summing up the three terms gives

$$\sum_{l_1, l_2} \begin{vmatrix} R(i_1, l_1) & R(i_1, l_2) \\ R(i_2, l_1) & R(i_2, l_2) \end{vmatrix}^2 = 2S(i_1, i_1)S(i_2, i_2) - S(i_1, i_2)^2 = 2 \begin{vmatrix} S(i_1, i_1) & S(i_1, i_2) \\ S(i_2, i_1) & S(i_2, i_2) \end{vmatrix}.$$

Adding the second double summation completes the proof. \square

References

- [1] Animashree Anandkumar, Kamalika Chaudhuri, Daniel J Hsu, Sham M Kakade, Le Song, and Tong Zhang. Spectral methods for learning multivariate latent tree structure. In *Advances in neural information processing systems*, pages 2025–2033, 2011.
- [2] Kevin Atteson. The performance of neighbor-joining methods of phylogenetic reconstruction. *Algorithmica*, 25(2-3):251–278, 1999.
- [3] Bernard P Brooks. The coefficients of the characteristic polynomial in terms of the eigenvalues and the elements of an $n \times n$ matrix. *Applied mathematics letters*, 19(6):511–515, 2006.
- [4] David Bryant. On the uniqueness of the selection criterion in neighbor-joining. *Journal of Classification*, 22(1):3–15, 2005.

REFERENCES

- [5] Joseph H Camin and Robert R Sokal. A method for deducing branching sequences in phylogeny. *Evolution*, 19(3):311–326, 1965.
- [6] Joseph T Chang. Full reconstruction of markov models on evolutionary trees: identifiability and consistency. *Mathematical biosciences*, 137(1):51–73, 1996.
- [7] Joseph T Chang and John A Hartigan. Reconstruction of evolutionary trees from pairwise distributions on current species. In *Computing science and statistics: Proceedings of the 23rd symposium on the interface*, pages 254–257. Interface Foundation Fairfax Station, VA, 1991.
- [8] William HE Day and David Sankoff. Computational complexity of inferring phylogenies by compatibility. *Systematic Biology*, 35(2):224–229, 1986.
- [9] Frédéric Delsuc, Henner Brinkmann, and Hervé Philippe. Phylogenomics and the reconstruction of the tree of life. *Nature Reviews Genetics*, 6(5):361, 2005.
- [10] Richard Durbin, Sean R Eddy, Anders Krogh, and Graeme Mitchison. *Biological sequence analysis: probabilistic models of proteins and nucleic acids*. Cambridge university press, 1998.
- [11] George F Estabrook, FR McMorris, and Christopher A Meacham. Comparison of undirected phylogenetic trees based on subtrees of four evolutionary units. *Systematic Zoology*, 34(2):193–200, 1985.
- [12] Joseph Felsenstein. Evolutionary trees from dna sequences: a maximum likelihood approach. *Journal of molecular evolution*, 17(6):368–376, 1981.
- [13] Joseph Felsenstein. *Inferring phylogenies*, volume 2. Sinauer associates Sunderland, MA, 2004.
- [14] Walter M Fitch. Toward defining the course of evolution: minimum change for a specific tree topology. *Systematic Biology*, 20(4):406–416, 1971.
- [15] Olivier Gascuel and Mike Steel. Neighbor-joining revealed. *Molecular biology and evolution*, 23(11):1997–2000, 2006.
- [16] Olivier Gascuel and Mike Steel. A stochastic safety radius for distance-based tree reconstruction. *Algorithmica*, 74(4):1386–1403, 2016.
- [17] Stéphane Guindon and Olivier Gascuel. A simple, fast, and accurate algorithm to estimate large phylogenies by maximum likelihood. *Systematic biology*, 52(5):696–704, 2003.
- [18] Mateja Hajdinjak, Qiaomei Fu, Alexander Hübner, Martin Petr, Fabrizio Mafessoni, Steffi Grote, Pontus Skoglund, Vagheesh Narasimham, Hélène Rougier, Isabelle Crevecoeur, et al. Reconstructing the genetic history of late neanderthals. *Nature*, 555(7698):652, 2018.
- [19] Stefan Harmeling and Christopher KI Williams. Greedy learning of binary latent trees. *IEEE Transactions on Pattern Analysis and Machine Intelligence*, 33(6):1087–1097, 2010.
- [20] Ariel Jaffe, Ethan Fetaya, Boaz Nadler, Tingting Jiang, and Yuval Kluger. Unsupervised ensemble learning with dependent classifiers. In *Artificial Intelligence and Statistics*, pages 351–360, 2016.
- [21] Ariel Jaffe, Boaz Nadler, and Yuval Kluger. Estimating the accuracies of multiple classifiers without labeled data. In *Artificial Intelligence and Statistics*, pages 407–415, 2015.

REFERENCES

- [22] Ariel Jaffe, Roi Weiss, Shai Carmi, Yuval Kluger, and Boaz Nadler. Learning binary latent variable models: A tensor eigenpair approach. *Proceedings of the 35th International Conference on International Conference on Machine Learning*, 2018.
- [23] Tao Jiang, Paul Kearney, and Ming Li. A polynomial time approximation scheme for inferring evolutionary trees from quartet topologies and its application. *SIAM Journal on Computing*, 30(6):1942–1961, 2001.
- [24] Katherine St John, Tandy Warnow, Bernard ME Moret, and Lisa Vawter. Performance study of phylogenetic methods:(unweighted) quartet methods and neighbor-joining. *Journal of Algorithms*, 48(1):173–193, 2003.
- [25] Thomas H Jukes, Charles R Cantor, et al. Evolution of protein molecules. *Mammalian protein metabolism*, 3(21):132, 1969.
- [26] Michelle R Lacey and Joseph T Chang. A signal-to-noise analysis of phylogeny estimation by neighbor-joining: insufficiency of polynomial length sequences. *Mathematical Biosciences*, 199(2):188–215, 2006.
- [27] James A Lake. Reconstructing evolutionary trees from dna and protein sequences: parilinear distances. *Proceedings of the National Academy of Sciences*, 91(4):1455–1459, 1994.
- [28] Robert S Lanciotti, Amy J Lambert, Mark Holodniy, Sonia Saavedra, and Leticia del Carmen Castillo Signor. Phylogeny of zika virus in western hemisphere, 2015. *Emerging infectious diseases*, 22(5):933, 2016.
- [29] Radu Mihaescu, Dan Levy, and Lior Pachter. Why neighbor-joining works. *Algorithmica*, 54(1):1–24, 2009.
- [30] Elchanan Mossel and Sébastien Roch. Learning nonsingular phylogenies and hidden markov models. In *Proceedings of the thirty-seventh annual ACM symposium on Theory of computing*, pages 366–375, 2005.
- [31] Raphaël Mourad, Christine Sinoquet, Nevin Lianwen Zhang, Tengfei Liu, and Philippe Leray. A survey on latent tree models and applications. *Journal of Artificial Intelligence Research*, 47:157–203, 2013.
- [32] Masatoshi Nei and Sudhir Kumar. *Molecular evolution and phylogenetics*. Oxford university press, 2000.
- [33] Fabio Parisi, Francesco Strino, Boaz Nadler, and Yuval Kluger. Ranking and combining multiple predictors without labeled data. *Proceedings of the National Academy of Sciences*, 111(4):1253–1258, 2014.
- [34] Yves Pauplin. Direct calculation of a tree length using a distance matrix. *Journal of Molecular Evolution*, 51(1):41–47, 2000.
- [35] Judea Pearl and Michael Tarsi. Structuring causal trees. *Journal of Complexity*, 2(1):60–77, 1986.
- [36] Bruce Rannala and Ziheng Yang. Probability distribution of molecular evolutionary trees: a new method of phylogenetic inference. *Journal of molecular evolution*, 43(3):304–311, 1996.

REFERENCES

- [37] Vincent Ranwez and Olivier Gascuel. Quartet-based phylogenetic inference: improvements and limits. *Molecular biology and evolution*, 18(6):1103–1116, 2001.
- [38] Sebastien Roch. A short proof that phylogenetic tree reconstruction by maximum likelihood is hard. *IEEE/ACM Transactions on Computational Biology and Bioinformatics*, 3(1):92–94, 2006.
- [39] Joseph P Rusinko and Brian Hipp. Invariant based quartet puzzling. *Algorithms for Molecular Biology*, 7(1):35, 2012.
- [40] Naruya Saitou and Masatoshi Nei. The neighbor-joining method: a new method for reconstructing phylogenetic trees. *Molecular biology and evolution*, 4(4):406–425, 1987.
- [41] Charles Semple, Mike Steel, et al. *Phylogenetics*, volume 24. Oxford University Press on Demand, 2003.
- [42] Andrew B Smith. Rooting molecular trees: problems and strategies. *Biological Journal of the Linnean Society*, 51(3):279–292, 1994.
- [43] Sagi Snir, Tandy Warnow, and Satish Rao. Short quartet puzzling: A new quartet-based phylogeny reconstruction algorithm. *Journal of Computational Biology*, 15(1):91–103, 2008.
- [44] Robert R Sokal. A statistical method for evaluating systematic relationships. *Univ. Kansas, Sci. Bull.*, 38:1409–1438, 1958.
- [45] Alexandros Stamatakis. Raxml-vi-hpc: maximum likelihood-based phylogenetic analyses with thousands of taxa and mixed models. *Bioinformatics*, 22(21):2688–2690, 2006.
- [46] Mike Steel. *Phylogeny: discrete and random processes in evolution*. SIAM, 2016.
- [47] Korbinian Strimmer and Arndt von Haeseler. Accuracy of neighbor joining for n-taxon trees. *Systematic biology*, 45(4):516–523, 1996.
- [48] Korbinian Strimmer and Arndt Von Haeseler. Quartet puzzling: a quartet maximum-likelihood method for reconstructing tree topologies. *Molecular biology and evolution*, 13(7):964–969, 1996.
- [49] Jeet Sukumaran and Mark T Holder. Dendropy: a python library for phylogenetic computing. *Bioinformatics*, 26(12):1569–1571, 2010.
- [50] Edward Susko, Yuji Inagaki, and Andrew J Roger. On inconsistency of the neighbor-joining, least squares, and minimum evolution estimation when substitution processes are incorrectly modeled. *Molecular biology and evolution*, 21(9):1629–1642, 2004.
- [51] Koichiro Tamura, Masatoshi Nei, and Sudhir Kumar. Prospects for inferring very large phylogenies by using the neighbor-joining method. *Proceedings of the National Academy of Sciences*, 101(30):11030–11035, 2004.
- [52] John Wakeley. *Coalescent theory: an introduction*. Number 575: 519.2 WAK. 2009.
- [53] Mark Wilkinson, James O McInerney, Robert P Hirt, Peter G Foster, and T Martin Embley. Of clades and clans: terms for phylogenetic relationships in unrooted trees. *Trends in ecology & evolution*, 22(3):114–115, 2007.
- [54] Ziheng Yang and Bruce Rannala. Molecular phylogenetics: principles and practice. *Nature reviews genetics*, 13(5):303, 2012.